ORIGINAL RESEARCH (AR) DOI: 10.4274/jems.2022.62534

Journal of ETA Maritime Science 2022;10(1):61-73

An Optimized Routing Procedure for Safe Navigation of Large Tankers in the Strait of Istanbul

Deniz Öztürk, Kadir Sarıöz

İstanbul Technical University, Department of Shipbuilding and Ocean Engineering, İstanbul, Turkey

Abstract

The risks associated with the navigation of large tankers in restricted waterways have resulted in continuing development of routing measures such as Traffic Separation Schemes (TSS). This is generally subject to discussion between the administration and ship operators which may find some navigational rules and regulations unnecessarily restrictive. Motivated by the need for an objective and scientific method to determine the vessel characteristics and environmental conditions for a safe passage through a restricted waterway, this paper presents an optimized routing procedure based on maneuvering simulations and non-linear direct search techniques which can be used to determine the best attainable route for large tankers in restricted waterways and specified environmental conditions. The mathematical model for predicting the maneuvering performance is based on a modular approach in which the hydrodynamic, propeller and rudder forces are computed separately, while environmental forces are estimated by semi-empirical methods. The objective of the optimization procedure is to determine the required number and magnitude of rudder control commands for remaining within a specified TSS and minimizing a grounding or collision possibility.

Keywords: Ship maneuvering, Route optimization, Traffic separation scheme, Strait of Istanbul

1. Introduction

Transportation of crude oil and refined petroleum products by tankers between production sites, refineries and points of consumption accounts for nearly a 30% of global [1]. These tankers are classified by their deadweight tonnage and the scale of economy dictates that the capacity should be as large as possible provided that there is adequate cargo oil to fill the tanks and sufficient loading/unloading facilities. As economic concerns resulted in classes of large tankers, the number of accidents, mainly due to the collision and grounding in restricted waterways, have created significant environmental, safety and financial risks [2]. Considering the environmental consequences, there is a possibility of damage to soil, water, air, and all living things in the ecosystem as a result of tanker accidents [3]. Also, safety is a crucial concern in securing the crew and passenger's lives as accidents lead to injury and, worse, loss of life [4]. From a financial point of view, these collisions can lead to unavoidable delays and reduction of profits [5]. These risks are not only associated with tanker size and cargo capacity but also strongly related to navigational conditions, environmental conditions, and crew competence. In studies where past tanker accidents were examined by risk analysis methods, navigation-based errors were expressed with sub-segments such as inefficient use of bridge navigation equipment, inappropriate route selection, and procedure failure [6]. Environmental factors are uncontrollable and can be considered as external effects such as weather conditions, traffic speed and density [7]. Besides, crew competence was examined in many studies within the context of the human factor, and it was revealed that competition in training, critical decision-making skills, and language skills can cause problems at sea [8,9]. In order to ease the problem, International Maritime Organization established vessel traffic control systems including traffic routing schemes, shipping lanes, speed limitations, etc. [10]. Traffic Separation Schemes (TSS) consisting of regulated traffic lanes indicating the traffic directions, turning-points,

Address for Correspondence: Deniz Öztürk, İstanbul Technical University, Department of Shipbuilding and Ocean Engineering, İstanbul, Turkey
E-mail: ozturkdeni@itu.edu.tr
ORCID ID: orcid.org/0000-0002-6694-3277

Received: 19.10.2021
Accepted: 03.03.2022

To cite this article: D. Öztürk and K. Sarıöz, "An Optimized Routing Procedure for Safe Navigation of Large Tankers in the Strait of Istanbul." *Journal of ETA Maritime Science*, vol. 10(1), pp. 61-73, 2022.

deep-water lanes, and separation zones between the main traffic lanes have proven to be very successful in preventing collisions and groundings in restricted waterways. Within the TSS the risk of collision or grounding will be reduced by avoiding the body of water between two opposite lanes and between the lane and the shoreline, respectively.

TSS is implemented to regulate shipping through the Turkish straits, consisting of the strait of Istanbul and the strait of Çanakkale since 1994 [2]. The Maritime Traffic Regulations for the Turkish Straits and the Marmara Region were revised in 1998 [11]. These instructions regulated the suspension of all traffic in conditions of poor visibility, the implementation of one-way traffic during the transit of certain types of vessels and the restriction of large vessels carrying hazardous cargo to daylight-only transit. It is assumed that some vessels because of their type, size or maneuvering characteristics could not navigate safely within the TSS. In the regulations, a vessel with restricted ability to maneuver in the TSS is defined as a vessel 150 meters in length or more carrying dangerous cargo such as crude oil. It should also be noted that ships that will be subject to additional rules for safe passage of the strait are defined as ships with an overall length of 300 meters and above, and misunderstandings can lead to dangerous situations and even accidents in the Turkish straits. The passage of such vessels is restricted to permitted daylight hours and they are not allowed to be in the straits at the same time in the opposite directions. Periods of poor weather also exacerbate the problem by further restricting passage within the permitted hours. So, significant delays are inevitable for transportation on restricted seaways. Also, the overcrowding of anchorages at the ends of the Strait of Istanbul, increasing the risk of collisions.

The length classification is mainly based on the pilot experiences and has been a matter of discussion between the ship operators and the regulatory bodies. For example, based on the experience of its members OCIMF [12] suggests that the Suezmax class tanker of 275 meters has the maximum size which can safely navigate the Strait of Istanbul with acceptable margins. Clearly, analytical techniques need to be developed for the navigational safety of large vessels in restricted waterways. Sariöz and Narli [13] used a real-time ship maneuvering simulation to assess the behavior of large vessels in a TSS under external forces. It was shown that depending on the ship master's skill and experience the maneuvering behavior of the vessel may differ significantly. This raises the question of whether a set of optimum engine and rudder control commands exist for a safe passage through a specified TSS for given environmental conditions. A simulation-based optimization method is developed by Gucma [14] for safe entering of bulk carriers with a 300-meter length for a specific commercial port. In order to improve safety in navigation, more followed work was done for hydrodynamic interaction of vessels in constrained waterways. Lee et al. [15] determined the minimum safe distance between two vessels and speed limitations numerically for a curved narrow channel. Shu et al. [16] also analyzed automated identification system data collected for a port to investigate the effects of not only ship encounters but also external factors on ship behavior. According to the typical maneuvers involved at confined waterway, Du et al. [17] proposed a numerical tool to investigate the maneuvering characteristics. Based on identified hydrodynamic coefficients, the authors indicated that fitting formulas are required to describe the turning phenomenon. In a restricted two-way waterway, Liu et al. [18] carried out a comprehensive traffic simulation model to be a guide to improve the efficiency in ship traffic. In the study, which stated that ship speed and channel length are the most critical factors, features such as navigational rules and interaction between ships were also included in the model. Another Very Large Crude Carriers (VLCC) maneuvering simulation through the strait of Istanbul was simulated by Bayezit et al. [19] to express the safety of autopilot mode. In the study, the one-way passage was examined and although the voyage was generally safe in the Strait of Istanbul, it was revealed that the controller parameters should be optimized to be successful in critical areas. VLCC models were also investigated in maneuvering performance perspective with different mathematical models [20]. As a result of the study, it is stated that the Maneuvering Modeling Group (MMG) model-based third-order polynomial has an advantage in terms of determining the maneuver characteristics.

In the simplest meaning, an optimization problem for ship routing consists of determining a proper value of a function by systematically selecting control parameters from within a set. Setting up a rational and accurate ship routing system by means of optimization procedures is important to provide effective management in navigation routes, and to determine traffic separation lanes. In the present paper, an optimized routing procedure based on ship maneuvering simulations and non-linear direct search techniques to yield an optimum set of propeller/rudder control commands for a safe passage through a specified TSS is presented. The maneuvering simulation procedure, as described in Section 2, is based on a modular mathematical model in which

hydrodynamic forces, propeller and rudder forces and the environmental effects are estimated in separate modules. Then, the non-linear equations of motion are solved in the time domain to predict the vessel trajectory for given engine RPM, rudder angle under specified conditions.

In order to validate the mathematical model, a typical VLCC designed by KRISO which is referred to as KVLCC2 by SIMMAN workshops was selected as a benchmark case [21]. The reason for focusing on the oil tanker in the current study is that oil tanker operations are extremely critical due to having potential risks. The collision or grounding of oil tankers has the greatest risks of fires or explosions, air pollution, and such environmental damages. Obviously, many ship types, including bulk carriers and container ships, use the Istanbul strait on a regular basis, in addition to oil tankers. It is expected that similar results would be obtained with different ship types of similar dimensions and sizes.

In Section 3, the turning and zig-zag tests were simulated and compared with the full-scale test results. Section 4 presents a numerical optimization procedure to determine the rudder control commands required for a safe passage through the lanes of the TSS established at the Straits of Istanbul. The procedure is based on an inverse approach: The maneuvering theory is recast in terms of the performance criteria defined as the deviation from a specified trajectory. Here, the propeller revolutions and the rudder angles are the values of the ship maneuvering control parameters.

2. Mathematical Maneuvering Model

The behavior of a vessel navigating in a seaway in the presence of wind, waves and current can be represented by a set of coupled non-linear differential equations in six degrees of freedom. However, for large vessels such as VLCC's the primary motions can be considered to take place in the horizontal plane and the heave, pitch and roll motions may be ignored, particularly in restricted waterways where the wave conditions are not severe.

The Earth-fixed and the body-fixed reference frames are shown in Figure 1. The origin of the body-fixed reference frame is located at the mid-ship and the x and y axes correspond to the longitudinal and lateral direction of the vessel, respectively. The ship's center of gravity is located at $(x_{OG}, y_{OG}, 0)$ in the system of coordinates. The path of the vessel is defined as the trajectory traced by the centre of gravity. Heading refers to the direction (ψ, yaw angle) of the ship's longitudinal axis with respect to the Earth-fixed longitudinal axis. The difference between the heading and the actual course (or direction of the velocity vector at the center of gravity) is the drift angle, β.

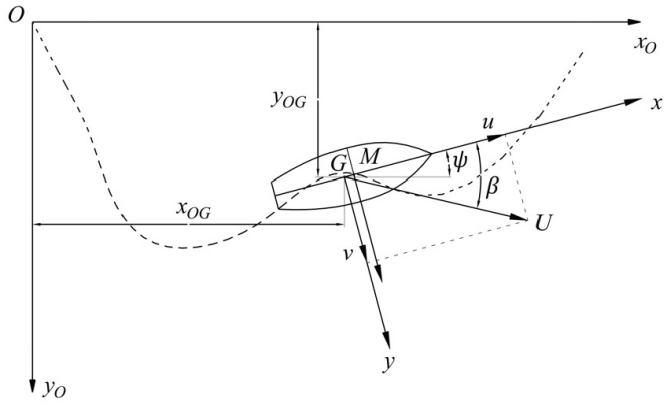

Figure 1. *Earth-fixed and ship-fixed coordinate systems*

The equations of motion for a ship moving in the horizontal plane with respect to a body-fixed reference frame can be derived as follows by using Newton's equation of motion;

$$\begin{aligned} &\text{Surge} && m(\dot{u} - vr - x_{OG}r^2) = X_H + X_P + X_R + X_{EXT} \\ &\text{Sway} && m(\dot{v} + ur + x_{OG}\dot{r}) = Y_H + Y_P + Y_R + Y_{EXT} \\ &\text{Yaw} && I_z\dot{r} + m x_{OG}(\dot{v} + ur) = N_H + N_P + N_R + N_{EXT} \end{aligned} \quad (1)$$

where

m	: mass of the ship
u, v	: ship velocities in x and y axes
$\dot{u}, \dot{v}$	: ship accelerations in x and y axes
$r, \dot{r}$	: yaw rate and acceleration
I_Z	: mass moment of inertia about vertical axis through the centre of gravity
X, Y	: surge and sway forces about longitudinal and lateral axes
N	: yaw moment about vertical axis through the centre of gravity
H, P, R, EXT	: subscripts indicating hull, propeller, rudder and external forces

This mathematical model is based on the concept of modularity which is achieved by isolating the forces exerted on the ship by the hull and appendages, rudder(s), propeller(s) and external forces. The basic mathematical modules required to solve the equations of motion for typical large surface vessels are related to the following:

• Hydrodynamic forces due to the hull and appendages (X_H, Y_H, N_H),

- Propulsion forces due to the propellers and thrusters (X_P, Y_P, N_P),
- Forces due to control surfaces like rudder and fins (X_R, Y_R, N_R),
- Forces due to the environmental disturbances such as wind, current and waves (X_{EXT}, Y_{EXT}, N_{EXT}).

2.1. Hydrodynamic Forces due to the Hull and Appendages

The prediction of hydrodynamic forces on a maneuvering vessel is a complex problem due primarily to the complications of viscous and free-surface effects. It will be assumed that the disturbance of free surface is sufficiently small and the hydrodynamic forces at any instant depend only on the prevailing instantaneous velocities and accelerations of the ship. Then, the hydrodynamic forces due to the hull and appendages can be considered as sum of two main components:

- Added mass and moment (inertia) components due to the motion in an ideal fluid with no circulation,
- Viscous damping force and moment components accounting primarily for viscous dissipative losses of a maneuvering ship.

2.1.1. Added Mass and Moment Components

The added mass and moment (inertia) components are important at the initial and transient parts of the ship maneuvering but the contribution of these terms in the steady or near steady part of the turning maneuver is small. Since the added mass and moment are assumed to be essentially the result of the inertia of the fluid they can be estimated using potential theory as a function of the hull geometry and the fluid density. The complete set equations for added mass and moment components can be simplified by assuming that there is no significant interaction between viscous and inertia properties of the fluid, and the second or higher order acceleration terms can be neglected. It may also be assumed that terms representing cross-coupling between acceleration and velocity parameters are zero or negligibly small, and forces and moments have appropriate port and starboard symmetry. Then the added mass and moment components can be expressed as follows:

$$X_I = \frac{\rho}{2} L^3 \left(X'_{\dot{u}} \dot{u}\right)$$

$$Y_I = \frac{\rho}{2} L^4 \left(Y'_{\dot{r}} \dot{r}\right) + \frac{\rho}{2} L^3 \left(Y'_{\dot{v}} \dot{v}\right) \quad (2)$$

$$N_I = \frac{\rho}{2} L^5 \left(N'_{\dot{r}} \dot{r}\right) + \frac{\rho}{2} L^4 \left(N'_{\dot{v}} \dot{v}\right)$$

The coefficients in these equations are known as the hydrodynamic/maneuvering derivatives. Typical examples of empirical methods to estimate the coefficients are presented below:

$$X'_{\dot{u}} = 0.55\, C_B \frac{B}{L} Y'_{\dot{v}}$$

$$Y'_{\dot{v}} = -\pi \left(\frac{T}{L}\right)^2 \left[1 + 0.16 \frac{C_B B}{T} - 5.1 \left(\frac{B}{L}\right)^2\right]$$

$$Y'_{\dot{r}} = -\pi \left(\frac{T}{L}\right)^2 \left[0.67 \frac{B}{L} - 0.0033 \left(\frac{B}{T}\right)^2\right] \quad (3)$$

$$N'_{\dot{v}} = -\pi \left(\frac{T}{L}\right)^2 \left[1.1 \frac{B}{L} - 0.041 \frac{B}{T}\right]$$

$$N'_{\dot{r}} = -\pi \left(\frac{T}{L}\right)^2 \left[\frac{1}{12} + \frac{1}{60} \frac{C_B B}{T} - \frac{1}{3} \frac{B}{L}\right]$$

given by [22], and [23], where, L, B, T and C_B represent the length, breadth, draught and the block coefficient of the vessel, respectively.

2.1.2. Viscous Damping Force Components

Viscous damping forces, due to the viscous dissipative losses, affect the flow around a maneuvering vessel in two distinct ways. At small drift angles, the ship can be viewed as a low aspect ratio lifting surface in the lateral plane, with the assumption that the lift force develops with the circulatory flow. At larger drift angles, a significant part of the forces is due to the cross-flow drag which is not linearly related to drift and yaw angle velocities. In typical ship maneuvering problems, both circulatory and cross-flow forces are present and equally important in all stages of a manoeuver. A convenient way of expressing viscous hydrodynamic forces is to employ a Taylor expansion consisting of linear and 3rd order components as follows:

$$X_V = \frac{\rho}{2} L^4 \left(X'_{rr} r^2\right) + \frac{\rho}{2} L^3 \left(X'_{vr} vr\right) + \frac{\rho}{2} L^2 \left(X'_{vv} v^2\right)$$

$$Y_V = \frac{\rho}{2} L^4 \left(Y'_{rrr} r^3\right) + \frac{\rho}{2} L^3 \left(Y'_r ur + Y'_{vvr} vvr + Y'_{vrr} vrr\right) + \frac{\rho}{2} L^2 \left(Y'_v uv + Y'_{vvv} v^3\right) \quad (4)$$

$$N_V = \frac{\rho}{2} L^5 \left(N'_{rrr} r^3\right) + \frac{\rho}{2} L^4 \left(N'_r ur + N'_{vvr} vvr + N'_{vrr} vrr\right) + \frac{\rho}{2} L^3 \left(N'_v uv + N'_{vvv} v^3\right)$$

Typical semi-empirical formulae for estimating the linear viscous hydrodynamic force coefficients are presented by [23]:

$$\begin{aligned} Y'_v &= -\pi\left(\frac{T}{L}\right)^2\left[1+0.4\frac{C_B B}{T}\right] \\ Y'_r &= \pi\left(\frac{T}{L}\right)^2\left[\frac{1}{2}-2.2\frac{B}{L}+0.08\frac{B}{T}\right] \\ N'_v &= -\pi\left(\frac{T}{L}\right)^2\left[\frac{1}{2}+2.4\frac{T}{L}\right] \\ N'_r &= -\pi\left(\frac{T}{L}\right)^2\left[\frac{1}{4}+0.039\frac{B}{T}-0.56\frac{B}{L}\right] \end{aligned} \tag{5}$$

The empirical methods to estimate the non-linear maneuvering derivatives is limited comparing to linear ones due to the complexity. The preferred methods, expressed in [22], are given as follows:

$$\begin{aligned} X'_{vv} &= 12\left\{0.07\left(\frac{B}{L}\right)^2\frac{T}{L}\left[1+0.8\left(\frac{T}{B}\right)\right]^2\right\} \\ X'_{vr} &= C_B Y'_v\left[1+0.28\left(1.7-\sqrt{\frac{C_B B}{T}}\right)\right] \\ X'_{rr} &= -0.07\left(\frac{B}{L}\right)^2\frac{T}{L}\left[1+0.8\left(\frac{T}{B}\right)\right]^2 \\ Y'_{vrr} &= Y'_v/2.5 \\ N'_{vrr} &= 0.5N'_v \end{aligned} \tag{6}$$

The remaining unknown variables are expressed by [24] as follows.

$$\begin{aligned} Y'_{vvv} &= -\left(1.281\frac{T}{L}+0.031\right) \\ Y'_{vvr} &= 0.628\frac{C_B B}{L}-0.066 \\ Y'_{rrr} &= 0.029\frac{C_B B}{L}-0.004 \\ N'_{vvv} &= 0.188\frac{T}{L}-0.01 \\ N'_{vvr} &= 0.178\frac{C_B B}{L}-0.037 \\ N'_{rrr} &= -\left(0.014\frac{C_B B}{L}-0.002\right) \end{aligned} \tag{7}$$

The total hydrodynamic force components are represented by the summation of the inertia and viscous terms:

$$\begin{aligned} X_H &= \frac{\rho}{2}L^4 X'_{rr} r^2+\frac{\rho}{2}L^3\left(X'_{\dot u}\dot u+X'_{vr} vr\right)+\frac{\rho}{2}L^2\left(X'_{vv} v^2\right) \\ Y_H &= \frac{\rho}{2}L^4\left(Y'_{\dot r}\dot r+Y'_{rrr} r^3\right)+\frac{\rho}{2}L^3\left(Y'_{\dot v}\dot v+Y'_r ur+\right. \\ &\quad \left. Y'_{vvr} vvr+Y'_{vrr} vrr\right)+\frac{\rho}{2}L^2\left(Y'_v uv+Y'_{vvv} v^3\right) \\ N_H &= \frac{\rho}{2}L^5\left(N'_{\dot r}\dot r+N'_{rrr} r^3\right)+\frac{\rho}{2}L^4\left(N'_{\dot v}\dot v+N'_r ur+\right. \\ &\quad \left. N'_{vvr} vvr+N'_{vrr} vrr\right)+\frac{\rho}{2}L^3\left(N'_v uv+N'_{vvv} v^3\right) \end{aligned} \tag{8}$$

The equations of motion can be written as below with all of the acceleration-related terms placed in the left-hand side and all the other terms placed in right-hand side.

$$\begin{aligned} \left(m-\frac{\rho}{2}L^3 X'_{\dot u}\right)\dot u &= F_X(v,r) \\ \left(m-\frac{\rho}{2}L^3 Y'_{\dot v}\right)\dot v+\left(m x_{OG}-\frac{\rho}{2}L^4 Y'_{\dot r}\right)\dot r &= F_Y(u,v,r) \\ \left(m x_{OG}-\frac{\rho}{2}L^4 N'_{\dot v}\right)\dot v+\left(I_z-\frac{\rho}{2}L^5 N'_{\dot r}\right)\dot r &= F_N(u,v,r) \end{aligned} \tag{9}$$

where

$$\begin{aligned} F_X(v,r) &= \frac{\rho}{2}L^2 X'_{vv} v^2+\left(m+\frac{\rho}{2}L^3 X'_{vr}\right)vr+ \\ &\quad \left(m x_G+\frac{\rho}{2}L^4 X'_{rr}\right)r^2 \\ F_Y(u,v,r) &= \frac{\rho}{2}L^4\left(Y'_{rrr} r^3\right)+\left(\frac{\rho}{2}L^3 Y'_r-m\right)ur+ \\ &\quad \frac{\rho}{2}L^3\left(Y'_{vvr} vvr+Y'_{vrr} vrr\right)+\frac{\rho}{2}L^2\left(Y'_v uv+Y'_{vvv} v^3\right) \\ F_N(u,v,r) &= \frac{\rho}{2}L^5\left(N'_{rrr} r^3\right)+\left(\frac{\rho}{2}L^4 N'_r-m x_G\right)ur+ \\ &\quad \frac{\rho}{2}L^4\left(N'_{vvr} vvr+N'_{vrr} vrr\right)+\frac{\rho}{2}L^3\left(N'_v uv+N'_{vvv} v^3\right) \end{aligned} \tag{10}$$

These system of ordinary differential equations can be presented in the following standard form:

$$\begin{bmatrix} m-\frac{\rho}{2}L^3 X'_{\dot u} & 0 & 0 \\ 0 & m-\frac{\rho}{2}L^3 Y'_{\dot v} & m x_G-\frac{\rho}{2}L^4 Y'_{\dot r} \\ 0 & m x_G-\frac{\rho}{2}L^4 N'_{\dot v} & I_z-\frac{\rho}{2}L^5 N'_{\dot r} \end{bmatrix}\begin{bmatrix}\dot u\\ \dot v\\ \dot r\end{bmatrix} = \begin{bmatrix} F_X(v,r)\\ F_Y(u,v,r)\\ F_N(u,v,r)\end{bmatrix} \tag{11}$$

The solution of the equation yields the surge, sway, and yaw accelerations. The longitudinal and lateral velocity components and the yaw rate can be obtained by the following integrations with respect to time:

$$u(t)=\int_0^t \dot u(t)dt \;;\; v(t)=\int_0^t \dot v(t)dt \;;\; r(t)=\int_0^t \dot r(t)dt \tag{12}$$

The velocity components in a global coordinate system can be obtained through the following transformation:

$$\begin{aligned} \dot{x}(t) &= u(t)\cos\psi(t) - v(t)\sin\psi(t) \\ \dot{y}(t) &= u(t)\sin\psi(t) + v(t)\cos\psi(t) \end{aligned} \tag{13}$$

where $\psi(t)$ is the yaw angle which can be obtained by the integration of yaw rate with respect to time:

$$\psi(t) = \int_0^t r(t)dt \tag{14}$$

The coordinates of the center of gravity of the vessel defines the trajectory.

$$x(t) = \int_0^t \dot{x}(t)dt \quad ; \quad y(t) = \int_0^t \dot{y}(t)dt \tag{15}$$

2.2. Propeller Forces

The propellers operate in a complex flow field at the stern of the ship. The exact numerical simulation of the interaction between the current due to the presence of the propeller and the flow through the propeller requires powerful computational resources. Therefore, most propeller design and analysis applications are also carried out by establishing more practical flow models. Also, prediction of the propeller forces is important for maneuvers and indirectly for rudder force modelling. The propeller produces a thrust in the negative x-direction in Earth-fixed coordinate system. This force can be non-dimensionalized by the nominal rotational speed nD and propeller net thrust force may be represented by

$$X_P = (1-t)\rho\, n_P^2\, D_P^4\, K_T(J_P) \tag{16}$$

where t is the thrust deduction fraction, n_P the propeller rotational rate and D_P the propeller diameter. The thrust coefficient, $K_T(J_P)$, can be estimated by using the open water test measurements of the propeller in terms of the advance number, J_P, which is expressed as:

$$J_P = \frac{u_P}{n_P D_P} = \frac{u(1-w_P)}{n_P D_P} \tag{17}$$

where u is the axial ship velocity and w_P is the Taylor wake fraction for the propeller behind the ship hull. For a manoeuvring vessel the following empirical formula is developed for estimating w_P based on model test data [25]:

$$w_P = w\exp\left(K_1 \beta_P^2\right) \tag{18}$$

where w is the wake fraction value is based on an average longitudinal velocity at the propeller for a ship in straight ahead motion and $K_1 = -4.0$ is a constant. The geometrical inflow angle at propeller position is defined as,

$$\beta_P = \beta - x'_P r' \tag{19}$$

where β is the drift angle, x'_P is the non-dimensionalized longitudinal location of the propeller by $x\,p/L$, and r' is the non-dimensionalized yaw rate by rL/U.

Values of the thrust deduction fraction (t) and the wake fraction (w) for various types of ship hulls and propellers in ahead motion are normally determined from model test data, with appropriate corrections for scale effects in order to apply the results to full-scale ships. When the experimental data are not available semi-empirical method of [26] may be used for estimating the coefficients.

2.3. Rudder Forces

The components of the hydrodynamic forces acting on the rudder are essentially in the same category as for a ship hull, also the interaction with the propeller slipstream and the effective angle of attack should be fully taken into account. For large single screw/rudder vessels, such as VLCCs the standard MMG formulation has been shown to correlate well with the experimental and full-scale test results [27]. The surge force, sway force, and yaw moment generated by the rudder are respectively expressed as:

$$\begin{aligned} X_R &= -F_N \sin\delta \\ Y_R &= -(1+a_H) F_N \cos\delta \\ N_R &= -(x_R + a_H x_H) F_N \cos\delta \end{aligned} \tag{20}$$

where x_R is the x-coordinate of the centre of lateral force and δ is the rudder angle. The position of additional lateral force, x_H, is taken as $-0.45L_{BP}$. The a_H coefficient is the rudder force increase factor and can be estimated as a function of the block coefficient as follows:

$$a_H = 0.62(C_B - 0.6) + 0.227 \tag{21}$$

The normal force on the rudder, F_N, can be approximated as

$$F_N = \frac{\rho}{2}\frac{6.13\lambda}{\lambda + 2.25} A_R U_R^2 \sin\alpha_R \tag{22}$$

where A_R is the rudder area and λ is the rudder aspect ratio. The rudder inflow speed and angle are defined as follows:

$$U_R = \sqrt{u_R^2 + v_R^2}$$
$$\alpha_R = \delta - \tan^{-1}\left(\frac{v_R}{u_R}\right) \cong \delta - \frac{v_R}{u_R} \quad (23)$$

The longitudinal inflow velocity component, u_R can be estimated by use of the axial momentum theory for an actuator disk.

$$u_R = \varepsilon u_A \sqrt{\eta \left[1 + K_M\left(\sqrt{1 + \frac{8}{\pi}\frac{K_T}{J_P^2}} - 1\right)\right]^2 + (1 - \eta)} \quad (24)$$

where u_A is the speed of advance, η is the ratio of propeller diameter to rudder span, K_M is a function of the axial position of the rudder relative to the propeller and it equals 0.5 at the point on the propeller centre and 1.0 at infinity for downstream. K_T is the thrust coefficient, and J is the advance constant. The function ε represents the ratio of wake fraction at rudder position to that at the propeller position where w_P is the wake fraction at propeller and w_R is the wake coefficient at rudder position.

$$\varepsilon = \frac{1 - w_R}{1 - w_P} \quad (25)$$

The lateral inflow velocity component in the, v_R can be expressed as follows:

$$v_R = U\gamma \beta_R \quad (26)$$

where U is the resultant ship speed, γ is the flow rectifying effect and β_R is the effective inflow angle to rudder. The flow rectifying effect due the ship's hull and the propeller can be expressed as [25],

$$\gamma = C_P C_S \quad (27)$$

The propeller flow-rectification coefficient, C_P, is given in the following form:

$$C_P = 1/\sqrt{1 + 0.6\eta(2 - 1.4s)s/(1 - s)^2}, \quad s = 1 - u(1 - w_P)/n_P P \quad (28)$$

where P is the propeller pitch ratio. The ship flow-rectification coefficient, C_S, is given in the following form:

$$C_S = \begin{cases} K_3 \beta_R & for\ \beta_R \le C_{SO}/K_3 \\ C_{SO} & for\ \beta_R > C_{SO}/K_3 \end{cases} \quad (29)$$

with $K_3 = 0.45$ and $C_{SO} = 0.5$. The effective inflow angle to rudder, β_R is defined as follows:

$$\beta_R = \beta - 2x'_R r' \quad (30)$$

where β is the hull drift angle, x'_P non-dimensionalized longitudinal position of the rudder by x_R/L, and r' the dimensionalized yaw rate by rL/U.

2.4. External Forces

Many types of external forces may affect the maneuvering performance of a ship such as wave, wind and current forces, bank effects, ship-ship interaction, mooring lines, fender forces and anchor forces, and wave forces. Within the context of the present study only the current effects, the wind and waves forces are considered.

2.4.1. Current Effects

The current forces depend on the absolute velocity and the direction of current as well as the vessel velocity. The relative current velocity components in the longitudinal and transverse directions through the water is expressed by:

$$U_{Cx} = U_C \cos \alpha_C - u$$
$$U_{Cy} = U_C \sin \alpha_C - v \quad (31)$$

where

U_C : absolute current velocity

α_C : current direction with respect to Earth-fixed coordinate system

u, v : velocity components of ship in x and y directions

2.4.2. Wind Forces

There are various empirical methods that can be used to determine wind loads [28]. In the first of these methods [28], empirical formulas giving the transverse and longitudinal wind forces and wind moment were derived by analyzing the results of the experiments with different types of commercial ship models in different model test laboratories. Besides, in the study of [29] transverse and longitudinal wind cross-sectional areas are included in the wind force components and wind moment calculations. In the proposed method for offshore platforms [30], the cross-sectional area exposed to the wind includes all elements above the waterline such as the superstructure, crane, and derrick. The details of the method used in this study are presented below [31].

The wind force calculations are based on a steady-state one-minute mean wind velocity measured at an elevation of 10 meters above the water surface. For wind velocities at a different elevation, adjustments to the equivalent 10-meter velocity can be made with the following formula:

$$U_w = u_w \left(\frac{10}{h}\right)^{1/7} \tag{32}$$

where

u_w : wind velocity at elevation, h

h : elevation above water surface

Since the wind speed is subject to gusts the one-minute mean value is converted to the hourly mean value by multiplying by 1.15. The wind forces and moment can be estimated by using the following standard formulations:

$$X_W = \frac{\rho_a}{2} U_{Wr}^2 A_T C_{Wx}(\alpha_{Wr})$$

$$Y_W = \frac{\rho_a}{2} U_{Wr}^2 A_L C_{Wy}(\alpha_{Wr}) \tag{33}$$

$$N_W = \frac{\rho_a}{2} U_{Wr}^2 A_L L_{BP} C_{Wn}(\alpha_{Wr})$$

where

X_W, Y_W : wind force in surge and sway

N_W : wind moment

C_{Wx}, C_{Wy}, C_{Wn} : wind coefficients for given wind directions

ρ_a : density of air (1.23 kg/m^3)

α_{Wr} : relative wind direction

A_T, A_L : transverse and longitudinal wind area

L_{BP} : length between perpendiculars

U_{Wr} is the instantaneous wind velocity including the ship's speed over the ground with the following longitudinal and transverse components:

$$U_{Wr} = \sqrt{U_{Wx}^2 + U_{Wy}^2}$$

$$U_{Wx} = U_W \cos \alpha_W - u \tag{34}$$

$$U_{Wy} = U_W \sin \alpha_W - v$$

where

U_W : wind velocity

α_W : wind direction with respect to Earth-fixed coordinate system

u, v : velocity components of ship in x and y directions

Then, the relative wind direction (α_{Wr}), i.e. the angle between the speed through the water and the ships heading can be expressed as follows:

$$\alpha_{Wr} = \arctan\left(U_{Wy} / U_{Wx}\right) - \psi \tag{35}$$

where ψ is the heading of the vessel. The wind coefficients (C_{Wx}, C_{Wy}, C_{Wn}) for given wind directions can be obtained by model tests or Computational Fluid Dynamics analysis. Alternatively, for early design studies, empirical coefficients based on regression analysis of model test data can be used.

2.4.3. Wave Forces

The waves affect a maneuvering ship in two ways;

- First-order oscillatory forces centered on the dominant wave encounter frequency,
- Second-order drift forces which consist of a steady component and a low-frequency component.

The first-order harmonic wave forces are much larger in magnitude compared with the second-order forces. However, the effect on the trajectory of a maneuvering vessel in a restricted waterway with limited wave heights may be ignored. Since the second-order low-frequency wave forces are also oscillatory with a mean about zero they may also be ignored. Therefore, only the second-order mean wave drift forces need to be taken into account in the maneuvering simulation procedure.

The second-order mean wave drift forces can be estimated from model tests but require a complicated measurement system design. Ankudinov and Jakobsen [32] derived the following empirical formulae by using a large number of model tests, for estimating mean wave drift force components and the wave drift moment:

$$X_{WD} = \left[0.0388\, \rho g B\, C_B\, H_{1/3}^2 \sin^2\left(\frac{T}{2\, H_{1/3}}\right)\right] \cos\beta$$

$$Y_{WD} = \left[0.0388\, \rho g\, L_{WL}\, H_{1/3}^2 \sin^2\left(\frac{T}{2\, H_{1/3}}\right)\right] \sin\beta \tag{36}$$

$$N_{WD} = \left[-0.125\, \rho g\, L_{WL}\, T H_{1/3}^2 \sin^2\left(\frac{T}{2\, H_{1/3}}\right)\right] \cos\beta \sin\beta - 0.03\, Y_{WD}\, L_{WL}$$

where

X_{WD}, Y_{WD} : wave drag force in surge and sway

N_{WD} : wave drag moment

L_{WL} : length of waterline

B : breadth of waterline

T : ship draught

C_B : ship block coefficient

$H_{1/3}$: significant wave height
β : wave direction
g : gravitational acceleration

3. Validation of the Maneuvering Prediction Procedure

To validate the mathematical maneuvering model presented in Section 2, turning and zig-zag maneuver tests were carried out for KVLCC2. The main particulars of the vessel are presented in Table 1.

Table 1. *Main particulars of KVLCC2 tanker*

Parameter	Symbol (units)	Value
Length between perpendiculars	L_{BP} (m)	320.0
Length of waterline	L_{WL} (m)	325.5
Beam	B (m)	58.0
Depth	D (m)	30.0
Draught	T (m)	20.8
Block coefficient	C_B (-)	0.8098
Midship section coefficient	C_M (-)	0.998
Longitudinal centre of buoyancy	LCB (%)	3.48 of L_{WL} (fwd)
Displacement volume	∇ (m3)	312622
No of propellers	NP (-)	1
No of blades	Z (-)	4
Propeller diameter	D_p (m)	9.86
Pitch ratio at 0.7R	P/D (-)	0.721
No of rudders	NR (-)	1
Movable rudder area	A_R (m2)	136.7
Rudder deflection rate	δ_r (deg/s)	2.34

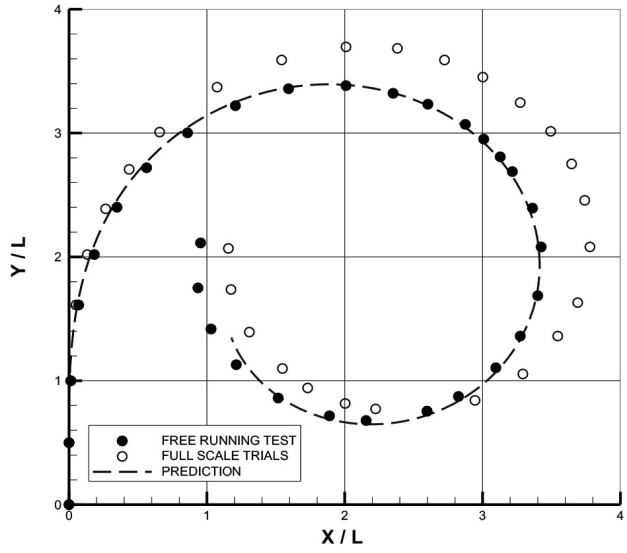

Figure 2. *Comparison of turning maneuvers for KVLCC2*

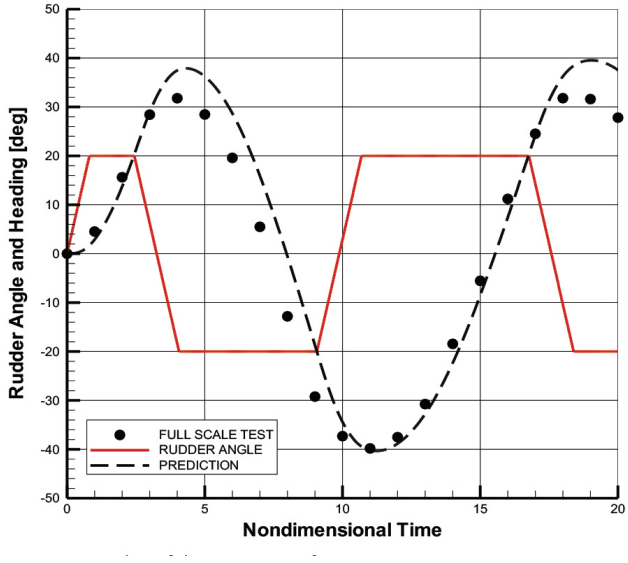

Figure 3. *Comparison of zig-zag maneuvers for KVLCC2*

A comparison of the turning circle maneuver for a rudder deflection angle, δ, of 35 degrees is shown in Figure 2. The turning simulation results are in excellent agreement with the free running test results. A similar comparison for the zig-zag maneuvering test is presented in Figure 3. It is clearly seen from these figures that the simulation results are in good agreement with the full-scale trial results. The trajectories of the vessel are plotted in MATLAB software.

4. Formulation of the Optimization Problem

This section presents a numerical optimization procedure to determine the rudder control commands required for a safe passage through the lanes of the TSS established at the Straits of Istanbul. The Strait of Istanbul lies between the Black Sea to the north, and the sea of Marmara to the south which is connected to the Mediterranean via the strait of Çanakkale. The length of the Strait of Istanbul is approximately 16.74 nautical miles, with an average width of 0.81 nautical miles. A major navigational difficulty in the Strait of Istanbul is the existence several sharp turns which require vessels to change course at least twelve times. At the narrowest point, Kandilli (700 m), a 45° course alteration is required.

In the present routing optimization approach, the theory is recast in terms of the performance criteria and the output of

the process are the values of the ship maneuvering control parameters, i.e. the propeller revolutions and the rudder angle. In order to simplify the problem, the propeller revolutions are assumed to be fixed at a value corresponding to a ship speed of 10 knots which is the maximum allowed speed by the administration [11]. The objective is to minimize the total deviation from the centerline of the traffic lane.

In general, a mathematical optimization problem can be described as follows:

Minimize $f(x)$

Subject to $g_i(x) \geq 0 \qquad i = 1,2,\ldots,m$

where $x = (x_1, x_2, \ldots, x_n)^T$ is the vector of optimisation variables. Thus the aim is to find the value of x that yields the best value of the objective function, $f(x)$, within a design space defined by the constraints, $g_i(x)$.

In the present routing optimization approach, the design variables x should be related to the rudder angle. It is assumed that the maximum rudder deflection angle is ±35° and the rudder can be deflected at intervals of 5 degrees, yielding a total of 15 optimization variables. In order to calculate the objective function, $f(x)$, the absolute value of the distance between the ship's center of gravity and the centerline of the traffic lane at each time step is computed and summed for the total simulation time to obtain a measure of merit representing the total deviation from the intended route. The vessel's position is determined by the coordinates of its center of gravity and the yaw angle which are calculated at each time step for the selected range of rudder angles. Then the total number of alternative trajectories is:

$$N_T = (n_R)^{n_T} \tag{37}$$

where, n_T is the number of time steps and n_R is the number of rudder angles. For a simulation of 6 minutes with a time step of 30 seconds and 15 rudder angles, the number of alternative trajectories would be about $N_T = (15)^{12} \cong 1.3 \times 10^{14}$. The evaluation of that many alternative trajectories requires an efficient optimization procedure. The non-linear direct search method of Hooke and Jeeves [33] has been found to work well for the problem under discussion.

In order to demonstrate the effectiveness of the developed numerical optimization procedure, several scenarios were investigated. To limit the simulation time only the most critical part of the Strait of Istanbul is considered. Only the loaded condition is taken into consideration because of the greater environmental risks. A matrix of simulation cases was defined in Table 2 so that the influence of different factors which affect the safety of navigation can be investigated independently.

As a first application the northbound VLCC in ideal environmental conditions case is considered. Note that, the northbound passage is defined as "N" and the southbound passage with "S" in Table 2. As shown in Figure 4a, the trajectory of the vessel is barely within the traffic lane while the swept track violates the boundaries. It should be reminded that this trajectory represent the best option among $N_T = (15)^{18} \cong 1.478 \times 10^{15}$ alternative trajectories, where 15 represents the number of possible rudder angles and 18 represents the simulation time of 9 minutes with a time step of 30 seconds. The time step of the simulation depends on the rudder deflection rate of the vessel. For the current VLCC the rudder deflection rate is 2.34 deg/s resulting in a 30 seconds time step to be able to change the rudder angle from -35° to +35°. The rudder deflection rate and the range of rudder angle may significantly affect the maneuvering performance of the vessel. For example, as shown in Figure 4b, when the range of rudder angle is limited to -20° to +20°, the vessel cannot remain within the traffic lane even in ideal environmental conditions.

In moderate environmental conditions represented by 3 knots current, 20 knots wind and 1-meter significant wave height, the best possible trajectory for the northbound VLCC in south-westerly winds for a maximum rudder angle of -35° to +35° is shown in Figure 5a. The drift forces due to the south-westerly winds, waves and current result in significant deviation from the centerline of the traffic lane and there is a strong possibility of a collision with a

Table 2. *Simulation matrix of KVLCC2 tanker at the Strait of Istanbul*

Passage	Velocity (knot)	Environmental condition	Wind (South West) (knot)	Current (South) (knot)	Wave height (South West) (m)	Rudder angle (°)	Increment (°)
N	10	Ideal	0	0	0	±35	5
N	10	Ideal	0	0	0	±20	5
N	10	Moderate	20	3	1	±35	5
N	10	Extreme	40	5	2	±35	5
S	10	Ideal	0	0	0	±35	5
S	10	Moderate	20	3	1	±35	5

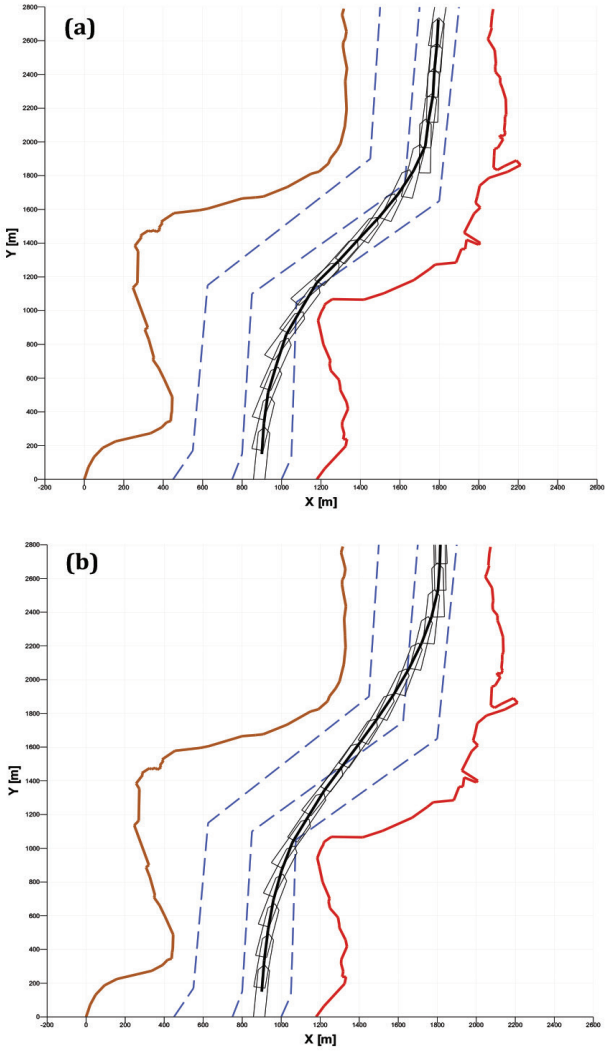

Figure 4. *Northbound VLCC, Ideal condition: (a) Maximum rudder angle: ±35°, (b) Maximum rudder angle: ±20°*

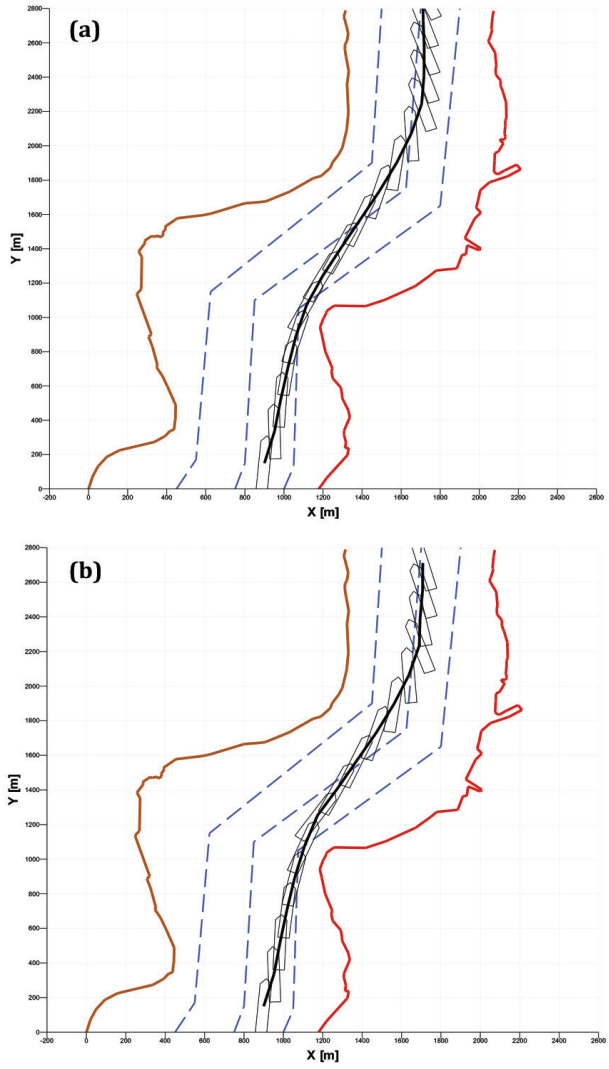

Figure 5. *Northbound VLCC, Maximum rudder angle: ±35°: (a) Moderate condition, (b) Extreme condition*

southbound vessel. In extreme environmental conditions, as shown in Figure 5b, the VLCC, even with the best possible rudder commands, could not remain within the boundaries of the traffic lane and a collision with a southbound vessel is inevitable. The best possible trajectories in ideal and moderate environmental conditions for the southbound VLCC are shown in Figure 6a and Figure 6b. Similar to the northbound VLCC, even in ideal environmental conditions, the southbound VLCC could barely navigate within the boundaries of the traffic line. In moderate environmental conditions, even with the best possible rudder commands, the vessel violates the traffic separation line resulting in a strong possibility of a collision with a northbound vessel.

5. Concluding Remarks

The main objective of the routing procedure is to determine the size of a vessel navigate within specified traffic lanes so that the possibility of a grounding or collision is minimized. An optimized ship routing procedure based on ship maneuvering simulations and non-linear direct search techniques has been developed and used to determine the best attainable route for large tankers in a restricted waterway, represented by the Strait of Istanbul, under the effects of specified environmental conditions. As a practical application, a typical VLCC was selected and the best attainable trajectories in the most critical part of the Strait of Istanbul were investigated. The major findings of these investigations are summarized as follows:

• Even under ideal conditions (no wind, no current, no wave) it is almost impossible for a typical VLCC to maintain its position within the traffic lanes in the critical part of the Strait of Istanbul. In order to prevent a collision or grounding, these type of vessels should not be allowed to be in the straits at the same time in the opposite directions

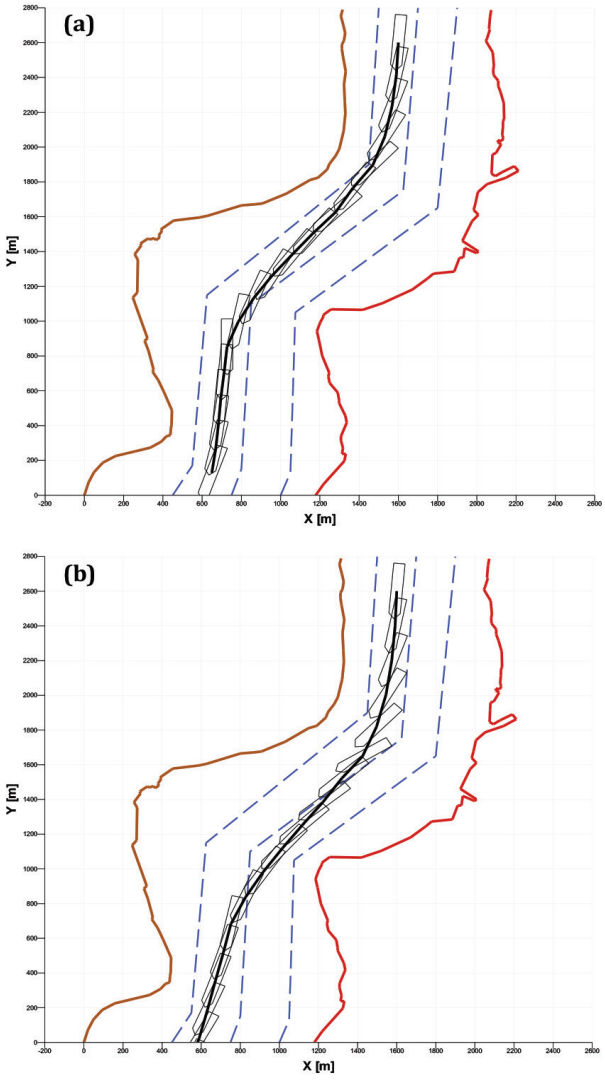

Figure 6. *Southbound VLCC, Maximum rudder angle: ±35°: (a) Ideal condition, (b) Moderate condition*

even under ideal environmental conditions.

• In moderate environmental conditions it is impossible for a typical VLCC to navigate through the critical part of the Strait of Istanbul without violating the traffic separation lanes. In such conditions only one-way traffic should be allowed to prevent collisions or grounding.

• In extreme environmental conditions, under strong winds and currents maintaining position within the lanes is not possible for typical VLCCs and they should not be allowed in the Strait of Istanbul until the environmental conditions are reduced to moderate levels.

Real time simulation of the maneuvering behavior of a vessel under the influence of wind, current and waves is such a complex mathematical problem that some simplifications are inevitable. In present study, the wind, current and wave effects are taken into account in a quasi-static manner. A fully-dynamic maneuvering simulation is a desired long-term research goal that needs sophisticated mathematical theories as well as extremely powerful computers. However, this tool could be further used to determine the ship particulars which can safely pass through a restricted waterway for specified or the maximum allowable environmental conditions.

Authorship Contributions

Concept design: K. Sarıöz, Data Collection or Processing: K. Sarıöz, Analysis or Interpretation: K. Sarıöz, Literature Review D. Öztürk, K. Sarıöz, Writing, Reviewing and Editing: D. Öztürk, K. Sarıöz.

Funding: The author(s) received no financial support for the research, authorship, and/or publication of this article.

References

[1] *UNCTAD Handbook of Statistics 2020 - Maritime transport indicators*. United Nations Publications, 2020. Available: https://unctad.org/system/files/official-document/tdstat45_FS15_en.pdf

[2] OCIMF, "Safety of Navigation through the Bosporus Strait, Sea of Marmara and Dardanelles, MSC 67/7/12," 1997.

[3] Y. S. Kim et al. "Environmental consequences associated with collisions involving double hull oil tanker," *Ships and Offshore Structures*, vol. 10, pp. 479-487, Apr 2015.

[4] P. Vidmar, and M. Perkovič, "Safety assessment of crude oil tankers," *Safety Science*, vol. 105, pp. 178-191, Jun 2018.

[5] Ö. Uğurlu, S. Erol, and E. Başar, "The analysis of life safety and economic loss in marine accidents occurring in the Turkish Straits," *Maritime Policy & Management*, vol. 43, pp. 356-370, 2016.

[6] Ö. Uğurlu, E. Köse, U. Yıldırım, and E. Yüksekyıldız, "Marine accident analysis for collision and grounding in oil tanker using FTA method," *Maritime Policy & Management*, vol. 42, pp. 163-185, 2015.

[7] J. Weng, S. Liao, B. Wu, and D. Yang, "Exploring effects of ship traffic characteristics and environmental conditions on ship collision frequency," *Maritime Policy & Management*, vol. 47, pp. 523-543, 2020.

[8] J. Mindykowski, "Impact of staff competences on power quality-related ship accidents," *2018 International Conference and Exposition on Electrical And Power Engineering (EPE)*, 2018, pp. 169-174.

[9] N. Berg, J. Storgård, and J. Lappalainen, *The Impact of Ship Crews on Maritime Safety*, 2013. https://www.merikotka.fi/wp-content/uploads/2018/08/Berg_TheImpactOfShipCrewsOnMaritimeSafety.pdf

[10] International Maritime Organization, *Ships' Routeing*. IMO, 2019. https://www.imo.org/en/OurWork/Safety/Pages/ShipsRouteing.aspx

[11] *Türk boğazları deniz trafik düzeni tüzüğü [Maritime traffic regulations for the Turkish straits]*. 1998, pp. 3497–3534. https://www.mevzuat.gov.tr/MevzuatMetin/2.5.9811860.pdf

[12] OCIMF, "Guidelines for Transiting the Turkish Straits," 2007. https://media.ellinikahoaxes.gr/uploads/2021/03/Guidelines-Turkist-Straits.pdf

[13] K. Sariöz, and E. Narli, "Assessment of manoeuvring performance of large tankers in restricted waterways: a real-time simulation approach," *Ocean Engineering*, vol. 30, pp. 1535-1551, Aug 2003.

[14] S. Gucma, "Optimization of Świnoujście port areas and approach channel parameters for safe operation of 300-meter bulk carriers," *Zeszyty Naukowe Akademii Morskiej w Szczecinie*, vol. 48, pp. 125-133, 2016.

[15] C. K. Lee, S. B. Moon, and T. G. Jeong, "The investigation of ship maneuvering with hydrodynamic effects between ships in curved narrow channel," *International Journal of Naval Architecture and Ocean Engineering*, vol. 8, pp. 102-109, Jan 2016.

[16] Y. Shu, W. Daamen, H. Ligteringen, and S. P. Hoogendoorn, "Influence of external conditions and vessel encounters on vessel behavior in ports and waterways using Automatic Identification System data," *Ocean Engineering*, vol. 131, pp. 1-14, Feb 2017.

[17] P. Du, A. Ouahsine, K. T. Toan, and P. Sergent, "Simulation of ship maneuvering in a confined waterway using a nonlinear model based on optimization techniques," *Ocean Engineering*, vol. 142, pp. 194-203, Sep 2017.

[18] K. Liu, X. Xin, J. Ma, J. Zhang, and Q. Yu, "Sensitivity analysis of ship traffic in restricted two-way waterways considering the impact of LNG carriers," *Ocean Engineering*, vol. 192, pp. 106556, Nov 2019.

[19] İ. Bayezit, R. Bitirgen, M. Hançer, and O. K. Kinaci, "Strait of İstanbul Crossing Simulation of a VLCC Type Ship in Autopilot Mode," *Journal of ETA Maritime Science*, vol. 7, pp. 304-316, 2019.

[20] E. Aksu, and E. Köse, "Evaluation of Mathematical Models for Tankers' Maneuvering Motions," *Journal of ETA Maritime Science*, vol. 5, pp. 95-109, 2017.

[21] F. Stern et al. "Experience from SIMMAN 2008-The first workshop on verification and validation of ship maneuvering simulation methods," *Journal of Ship Research*, vol. 55, pp. 135-147, Jun 2011.

[22] V. Ankudinov, "Ship Maneuvering Simulation Model Including Regimes of Slow Speeds and Large Drift Angles," in *First Maritime Simulation Symposium*, 1985.

[23] D. Clarke, P. Gedling, and G. Hine, "The Application of Manoeuvring Criteria in Hull Design Using Linear Theory," *Transactions of the Royal Institution of Naval Architects, RINA*, 1982.

[24] T. I. Lee, K. S. Ahn, H. S. Lee, and D. J. Yum, "On an empirical prediction of hydrodynamic coefficients for modern ship hulls," in *Proceedings of MARSIM'03*, 2003.

[25] S. Inoue, M. Hirano, K. Kijima, and J. Takashima, "A Practical Calculation Method of Ship Maneuvering Motion," *International Shipbuilding Progress*, vol. 28, pp. 207-222, Sep 1981.

[26] J. Holtrop, and G. G. J. Mennen, "An approximate power prediction method," *International Shipbuilding Progress*, vol. 29, pp. 166-170, Jul 1982.

[27] H. Yasukawa and Y. Yoshimura, "Introduction of MMG standard method for ship maneuvering predictions," *Journal of Marine Science and Technology*, vol. 20, pp. 37-52, Mar 2015.

[28] R. M. Isherwood, "Wind Resistance of Merchant Ships," *The Royal Institution of Naval Architects,* vol. 115. pp. 327-338, 1972.

[29] G. F. M. Remery, and G. Van Oortmerssen, "The mean wave, wind and current forces on offshore structures and their role in the design of mooring systems," in *Proceedings of the Annual Offshore Technology Conference*, 1973.

[30] American Petroleum Institute (API), *API Recommended Practice 2SK, Design and Analysis of Stationkeeping Systems for Floating Structures*, Third. 2008.

[31] Oil Companies International Marine Forum (OCIMF), *Prediction of Wind and Current Loads on VLCCs*, Second ed., 1994.

[32] V. Ankudinov and B. K. Jakobsen, "Wave Drift Forces in Shallow Water," 1990.

[33] R. Hooke, and T. A. Jeeves, "'Direct Search' Solution of Numerical and Statistical Problems," *Journal of the ACM*, vol. 8, pp. 212-229, 1961.